MEDICAL SCIENCE MONITOR

CLINICAL RESEARCH

e-ISSN 1643-3750
© Med Sci Monit, 2020; 26: e920754
DOI: 10.12659/MSM.920754

Received: 2019.10.16
Accepted: 2019.12.06
Available online: 2020.01.22
Published: 2020.03.06

Identification of 2 Potential Core Genes for Influence of Gut Probiotics on Formation of Intracranial Aneurysms by Bioinformatics Analysis

Authors' Contribution:
Study Design A
Data Collection B
Statistical Analysis C
Data Interpretation D
Manuscript Preparation E
Literature Search F
Funds Collection G

ABCDEF 1 Heng-Jian Liu*
EFG 2 Huan-Ting Li*
BC 1 Yuan Lin
C 1 Dong-Lin Lu
F 1 Yong Yue
E 1 Jing Xiong
D 1 Cong-Qin Li
C 1 Xiang-Yu Xu
AG 2 Yu-Gong Feng

1 Qingdao University, Qingdao, Shandong, P.R. China
2 Department of Neurosurgery, Affiliated Hospital of Qingdao University, Qingdao, Shandong, P.R. China

* Heng-Jian Liu and Huan-Ting Li contributed equally to this work

Corresponding Author: Yu-Gong Feng: e-mail: fengyugongqdu@163.com
Source of support: This work was financed by a grant-in-aid for scientific research from the National Natural Science Foundation of China (No. 81870914)

Background: Rupture of intracranial aneurysms (IA) is associated with high rates of mortality around the world. Use of intestinal probiotics can regulate the pathophysiology of aneurysms, but the details of the mechanism involved have been unclear.

Material/Methods: The GEO2R analysis website was used to detect the DEGs between IAs, AAAs, samples after supplementation with probiotics, and normal samples. The online tool DAVID provides functional classification and annotation analyses of associated genes, including GO and KEGG pathway. PPI of these DEGs was analyzed based on the STRING database, followed by analysis using Cytoscape software.

Results: We found 170 intersecting DEGs (contained in GSE75240 and more than 2 of the 4 aneurysms datasets), 5 intersecting DEGs (contained in all datasets) and 1 intersecting DEG (contained in GSE75240 and all IAs datasets). GO analysis results suggested that the DEGs primarily participate in signal transduction, cell adhesion, immune response, response to drug, extracellular matrix organization, cell-cell signaling, and inflammatory response in the BP terms, and the KEGG pathways are mainly enriched in focal adhesion, cytokine-cytokine receptor interaction, ECM-receptor interaction, amoebiasis, chemokine signaling pathway, proteoglycans, and PI3K-Akt signaling pathway in cancer pathways. Through PPI network analysis, we confirmed 2 candidates for further study: CAV1 and MYH11. These downregulated DEGs are associated with the formation of aneurysms, and the change of these DEGs is the opposite in probiotics-treated animals.

Conclusions: Our study suggests that MYH11 and CAV1 are potential target genes for prevention of aneurysms. Further experiments are needed to verify these findings.

MeSH Keywords: Blood • Intracranial Aneurysm • Probiotics

Full-text PDF: https://www.medscimonit.com/abstract/index/idArt/920754

Indexed in: [Current Contents/Clinical Medicine] [SCI Expanded] [ISI Alerting System] [ISI Journals Master List] [Index Medicus/MEDLINE] [EMBASE/Excerpta Medica] [Chemical Abstracts/CAS]

Background

Intracranial aneurysms (IAs) are the abnormal bulging that occurs on the wall of the artery. It is an important cause of spontaneous subarachnoid hemorrhage (SAH) [1]. In the past few years, hypertension, smoking, atherosclerosis, and other factors were shown to lead to the development and occurrence of aneurysms. Recently, many scholars have come to believe that congenital defects also affect the formation of aneurysms [2]. Pathological conditions and inflammation that alter the morphologies of the vasculature can activate vascular remodeling, including stenosis and vascular weakening [3,4]. Intestinal probiotics are an important group of bacteria that regulate homeostasis of the internal body environment. Recent studies have shown that gut probiotics affect various diseases and impact inflammation, which plays a considerable role in determining the severity and course of disease [5,6]. Findings indicate that intestinal probiotics can affect the pathological condition of aneurysms by regulating vascular inflammation [7]. With the rapid development of gene chip technologies, the Gene Expression Omnibus (GEO) has gradually come to play a significant role in bioinformatic analysis. In this research, we used bioinformatics analysis to discover potential core genes affected by gut probiotics that play a role in the formation of IAs, which may ultimately provide potential therapeutic targets.

Material and Methods

Acquisition of the gene expression datasets

The gene expression datasets were acquired from the GEO database (*https://www.ncbi.nlm.nih.gov/geo/*). Three gene expression profiles (GSE26969, GSE75436, and GSE54083) of IAs, 1 gene expression profile (GSE7084) of abdominal aortic aneurysm, and 1 gene expression profile (GSE75240) after supplementation with probiotics were selected. Among them, GSE26969 and GSE75436 were based on platform GPL570([HG-U133_Plus_2] Affymetrix Human Genome U133 Plus 2.0 Array), GSE54083 was based on platform GPL4133(Agilent-014850 Whole Human Genome Microarray 4x44K G4112F), GSE7084 was based on platform GPL2507 (Sentrix Human-6 Expression BeadChip), and GSE75240 was based on platform GPL11649 (Agilent-023647 B. Taurus (Bovine) Oligo Microarray v2). The GSE26969 dataset was submitted by Li et al., including 3 IAs samples and 3 normal superficial temporal artery (STAs) samples [8]. The GSE75436 dataset was submitted by Yu et al., including 15 IAs tissues and 15 STAs tissues. The GSE54083 dataset was submitted by Inoue, including 5 unruptured intracranial aneurysms (UIAs) and 10 STAs samples [9]. The microarray data of GSE7084 was submitted by Tromp, which consisted of 8 abdominal aortas and 7 abdominal aortic aneurysms (AAAs) [10]. The microarray data of GSE75240 was submitted by Worku, which consisted of 4 whole-blood samples collected at the beginning (Day 0) and end of the study (Day 60) after supplementation with probiotics [11].

Identification of DEGs

The GEO2R analysis website (*https://www.ncbi.nlm.nih.gov/geo/geo2r/*) was used to find differentially expressed genes (DEGs) between IAs and normal samples, AAAs and normal samples, or sample after supplementation with probiotics and normal samples. The P-values and Benjamini & Hochberg (false discovery rate) were applied to provide a balance between discovery of statistically significant genes and limitations of false-positives [12]. Probe sets without corresponding gene symbols or genes with more than 1 probe set were removed or we took the highest value of the absolute value, respectively. Subsequently, the |log fold change (FC)| and P-value were calculated [13]. The cut-off criteria for defining DEGs were P-value <0.05 and |logFC| ≥1.5. Statistical analysis was further evaluated for each dataset, and the significative DEGs was exhibited using the Venn diagram online analysis tool (bioinformatics.psb.ugent.be/webtools/Venn/) and the TBtoolsv0.6654 software.

GO and KEGG pathway analysis of DEGs

To study DEGs at a functional level, Kyoto Encyclopedia of Genes and Genomes (KEGG) pathway enrichment analysis and Gene Ontology (GO) analysis were analyzed and exhibited using the online biological analysis tool (DAVID version 6.8, *https://david.ncifcrf.gov/*), database for the annotation, visualization, and integrated discovery, which provides functional classification and annotation analyses of DEGs [14]. GO analysis is an available method for large-scale functional enrichment research and can be classified into biological process (BP), cellular component (CC), and molecular function (MF). KEGG pathway enrichment analysis includes biological pathways, diseases, chemical, genomes, and metabolic information. The corrected P-value <0.05 was regarded as a statistically significant difference, and the top 5 counts of GOs and KEGGs were selected.

PPI network construction and module analysis

The Search Tool for the Retrieval of Interacting Genes (STRING) version 11.0 database (*http://string-db.org/*) is designed to explore protein–protein interactions (PPI) [15]. The DEGs identified previously were first mapped to the STRING database. Only the interactions with a combined score ≥0.4 were considered as significant. Subsequently, the PPI network was visualized using Cytoscape 3.6.1 software, which was used with

Indexed in: [Current Contents/Clinical Medicine] [SCI Expanded] [ISI Alerting System] [ISI Journals Master List] [Index Medicus/MEDLINE] [EMBASE/Excerpta Medica] [Chemical Abstracts/CAS]

the maximal clique centrality (MCC) method to explore the PPI network for hub genes. We performed quantitative expression analysis of 30 candidate genes that could better explain the reliability of the results [16].

Results

Identification of significantly DEGs (associated with aneurysms or IAs)

Three datasets of IAs-related gene expression profiles (GSE26969, GSE54083, and GSE75436) were collected from the GEO database via GEO2R. One dataset of AAAs-related gene expression profiles (GSE7084) and probiotics-related gene expression profiles (GSE75240) were also downloaded from the GEO database. We set $|\log_2$ fold change (FC)$| \geq 1.5$ and P-value<0.05 as the criterion to identify significantly DEGs. We found 1398, 1372, 1807, 592, and 6233 significantly DEGs in the GSE26969, GSE54083, GSE75436, GSE7084, and GSE75240 datasets, respectively (Figures 1, 2). By using the Venn diagram webtool, we found that some DEGs about probiotics were associated with aneurysms formation, including 170 intersecting (contain GSE75240 and more than 2 of the 4 aneurysms datasets), 28 intersecting DEGs (contain GSE75240 and more than 3 of the 4 aneurysms datasets), 5 intersecting DEGs (contain all datasets), 70 intersecting DEGs (contain GSE75240 and more than 2 of the 3 IAs datasets), and 1 intersecting DEG (contain GSE75240 and all IAs datasets). These different groups were exhibited using the Venn diagram webtool and the TBtools v0.6654 software, including 6, 39, 53, 30, 167 upregulated and 80, 20, 75, 70, 3 downregulated genes in the 170 intersecting DEGs (GSE26969, GSE54083, GSE75436, GSE7084, and GSE75240 datasets) (Table 1, Supplementary Table 1). The 5 intersecting DEGs associated with aneurysms and probiotics were Cofilin 2 (CFL2), LIM domain containing preferred translocation partner in lipoma (LPP), Myosin Heavy Chain 11 (MYH11), Monoamine Oxidase B (MAOB), and MAS-Related GPR Family Member F (MRGPRF). One intersecting DEG associated with IAs and probiotics was caveolin 1 (CAV1). These 6 intersecting DEGs were distributed in different parts of the chromosome (Supplementary Figure 1).

Functional and pathway enrichment analyses of DEGs

Three terms of GO functional annotation analysis were analyzed and exhibited on these 170 intersecting DEGs mentioned above, including biological process (BP), cellular component (CC), and molecular function (MF). With a threshold of P-value <0.05, the DEGs were enriched in 115 GO terms and 12 KEGG pathways (Figure 3). The enriched GO functions for these DEGs showed the most significant terms were signal transduction, cell adhesion, immune response, extracellular matrix organization, cell–cell signaling, and inflammatory response in the BP term. These DEGs were enriched in plasma membrane, extracellular exosome, extracellular space, extracellular region, and membrane in the CC term, and these DEGs were enriched in protein binding, identical protein binding, calcium ion binding, heparin binding, and actin binding in the MF term. In the above GOs analysis, CFL2 was enriched in extracellular exosome, extracellular space, and protein binding. LPP was enriched in cell adhesion, plasma membrane, and protein binding. MYH11 was enriched in extracellular exosome and protein binding. MAOB was enriched in response to drug and extracellular exosome. MRGPRF was enriched in plasma membrane and extracellular exosome. CAV1 was mainly involved in plasma membrane, membrane, protein binding, and identical protein binding. Subsequently, we conducted KEGG pathway enrichment analysis. The enriched KEGG pathways mainly contained focal adhesion, cytokine-cytokine receptor interaction, amoebiasis, ECM-receptor interaction, chemokine signaling pathway, proteoglycans, and PI3K-Akt signaling pathway. These results demonstrate that CAV1 plays a central role in the focal adhesion and proteoglycans in cancer pathways.

Construction and analysis of PPI network

The PPI networks of 170 DEGs were analyzed using the STRING database. The subset of 170 DEGs with 319 interactions was included in the PPI network. In addition, those interactions were constructed by using Cytoscape software. The top 30 DEGs according to the MCC method were identified using the CytoHubba plugin and were ordered as follows: FN1, IGFBP5, APOE, LAMC1, CP, SPARCL1, IGFBP7, CHRDL1, COL1A1, TIMP3, COL1A2, FBLN1, THBS2, COL11A1, CCR5, CCL4, CXCL16, CXCL5, CCL19, CXCL14, TAGLN, CAV1, MYH11, MMP1, ESR1, MGP, FLNA, ADAMTS1, AGTR1, and HSP90AA1 (Table 2). Notably, CAV1 and MYH11 were included in these 30 DEGs. Through PPI network, we found genes that were tightly bound to CFL2, LPP, MYH11, MAOB, MRGPRF, and CAV1 in different GEO datasets (Figure 4). The Heatmap and PPI network clearly display that CFL2 and MYH11 were upregulated in GSE75240 and downregulated in GSE26969, GSE75436, and GSE7084. LPP, MAOB, and MRGPRF were upregulated in GSE75240 and downregulated in GSE26969, GSE75436, GSE7084, and GSE54083. CAV1 was upregulated in GSE75240 and downregulated in GSE26969 and GSE75436 (Table 3, Figures 4, 5). In general, these genes were basically increased in the formation of aneurysms, while the expression was decreased in probiotics. We also found that FLNA was strongly correlated with CAV1, CFL2, LPP, and MYH11 (Table 4).

Discussion

The rupture of IAs can cause serious SAH, which has significant socioeconomic implications. Many factors affect the formation

Indexed in: [Current Contents/Clinical Medicine] [SCI Expanded] [ISI Alerting System] [ISI Journals Master List] [Index Medicus/MEDLINE] [EMBASE/Excerpta Medica] [Chemical Abstracts/CAS]

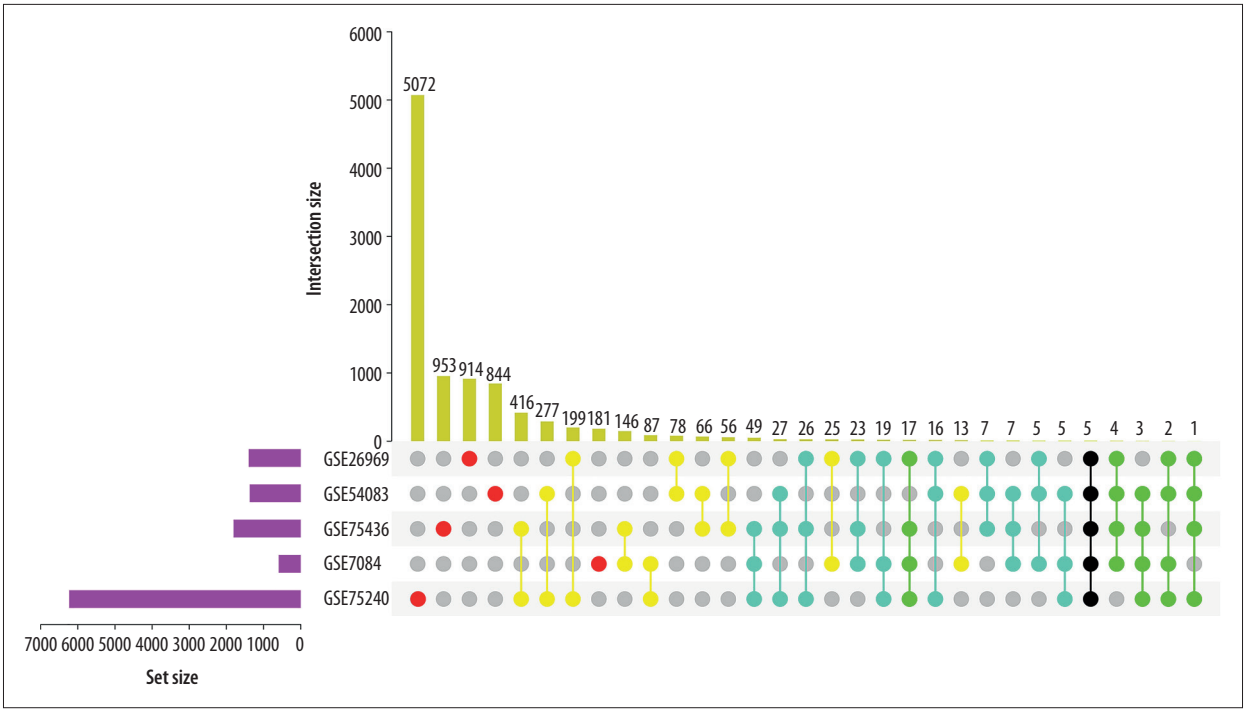

Figure 1. UpSet Plot analysis of DGEs. Red: in one dataset; yellow: in two datasets; Blue: in three datasets; green: in four datasets; Black: in five datasets

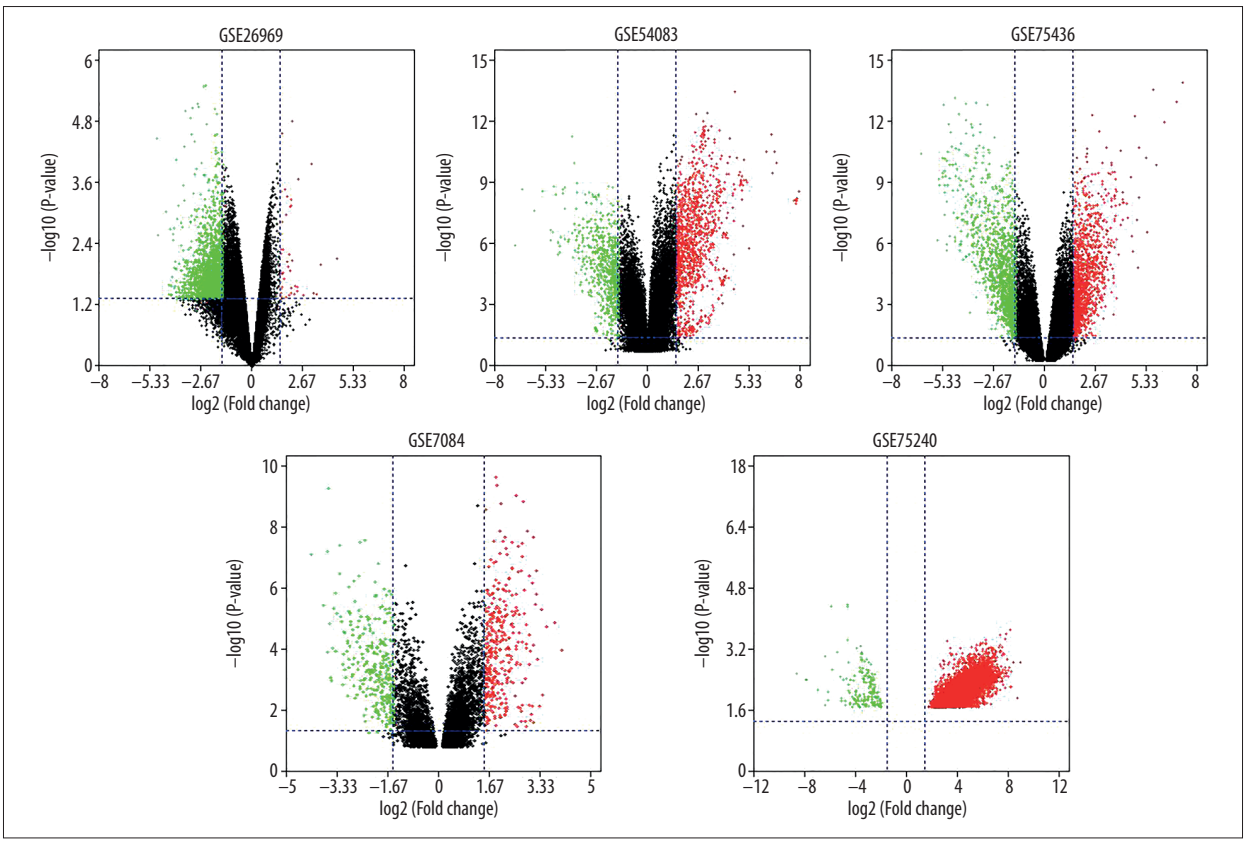

Figure 2. Volcano plot of DGEs. Red: up-regulation with fold change of more than 1.5; Green: down-regulation with a fold change of more than 1.5; Black: unchanged genes.

Indexed in: [Current Contents/Clinical Medicine] [SCI Expanded] [ISI Alerting System] [ISI Journals Master List] [Index Medicus/MEDLINE] [EMBASE/Excerpta Medica] [Chemical Abstracts/CAS]

Table 1. Intersecting DEGs.

Names	Total	Elements
GSE26969, GSE54083, GSE7084, GSE75240, GSE75436	5	CFL2, LPP, MYH11, MAOB, MRGPRF
GSE26969, GSE54083, GSE7084, GSE75436	4	RERG, ACTG2, SBSPON, CPED1
GSE26969, GSE54083, GSE7084, GSE75240	2	SORBS1, FBLN1
GSE26969, GSE7084, GSE75240, GSE75436	17	SYNM, PLN, PDGFD, KCNAB1, FHL5, SORBS2, KANK1, PRUNE2, CSRP2, INPP5A, ZAK, PPP1R14A, CNN1, CSRP1, AOC3, LMOD1, TAGLN
GSE54083, GSE7084, GSE75240, GSE75436	3	AIF1L, LTBP2, NUP210
GSE26969, GSE54083, GSE75240, GSE75436	1	CAV1
GSE26969, GSE54083, GSE7084	5	KLHL42, ADH5, MYL9, AIM1, JCHAIN
GSE26969, GSE7084, GSE75436	23	MAOA, RERGL, ADIRF, PALLD, HLA-DRA, PTPRC, SMTN, C11orf96, C2orf40, SYNPO2, FAM129A, RNASET2, DSTN, CCDC3, FILIP1L, EGR2, HLA-DMA, MYLK, EVI2B, MFAP4, NEXN, ADH1B, ACTA2
GSE26969, GSE7084, GSE75240	19	PLSCR4, SMOC2, SRPX, CAV2, IGFBP7, TMEM47, GPX3, SERPING1, TGFBR3, TCEAL4, PDLIM3, CPE, HSPB8, RGS5, SPARCL1, IGFBP5, RNASE1, CYBRD1, LAMC1
GSE54083, GSE7084, GSE75436	7	ACTC1, SLC43A2, TREM2, HMOX1, IL1B, HLA-DQB1, COTL1
GSE54083, GSE7084, GSE75240	5	PIK3CD, EFHD1, ERRFI1, MYH10, CXCL5
GSE7084, GSE75240, GSE75436	49	SLCO2B1, ACADL, RBPMS, ALOX5AP, SCARA3, IL10RA, CLEC5A, MPEG1, CKMT2, TIMP4, FLVCR2, MRAP2, KCNA5, NOV, GDF15, CD300A, MMP12, SLC37A2, APOD, IL1RN, FXYD1, RCAN2, ALDH1B1, TSPAN33, AGTR1, THBS2, CD300LF, CCR5, IRF8, KCNMA1, WISP2, APOE, CD8A, IGFBP2, MGP, MMP1, MYOC, CD4, SNX10, LMO3, PNKD, GLDN, CCL4, CD14, DEF6, BCL11A, PLAC8, CXCL16, CP
GSE26969, GSE54083, GSE75436	7	SLMAP, LOX, PDLIM5, IGHM, IGHA2///IGHA1///IGH, ENTPD4, TNC
GSE26969, GSE54083, GSE75240	16	AKR1B10, RAB14, LRRC40, DIXDC1, MAP3K7, HSP90AA1, RPS17, TIMP3, FGB, PDCD7, PRKAR2B, PNN, CFL1, ANKRD44, PNPLA8, NMD3
GSE26969, GSE75240, GSE75436	26	COL1A1, NEGR1, COL11A1, CHRDL1, PRR11, HNRNPC, SFRP1, TMTC1, MPP7, CLDND1, ADAMTS1, CDH11, PDE5A, PGM5, COL1A2, CXCL14, CD36, GREM1, CRISPLD2, FILIP1, ANGPTL1, ACACB, RASSF3, DES, NUP54, FLNA
GSE54083, GSE75240, GSE75436	27	CCL19, ROR2, IGSF11, PPARGC1A, FGF12, RHAG, ZNF280B, GPRIN3, FN1, GNAO1, NGFR, ESR1, CLEC7A, SGSM1, SULT1E1, GABRA4, GALNT3, CHST11, NRAP, TMEM169, PMP2, MSR1, IGSF21, NETO2, SMPDL3A, CTNNA3, STAC

of aneurysms by altering hemodynamics and morphologies of the cerebral vasculature. Intestinal probiotics can regulate homeostasis of the internal body environment. Recent studies showed that gut microbiota affect the pathological condition of aneurysms by modulating the immune system [5,6]. Understanding the molecular mechanism of probiotics in reducing aneurysms formation is of vital clinical significance for diagnosis and treatment.

More than 300 scientists from 25 countries eventually came to the conclusion that the cattle genome contain at least 22 000 protein-coding genes and the genetic similarity between cattle and humans is 80%, which is greater than that between humans and mice or rats [17]. This means that cattle can replace mice or rats as animal models of human disease. Some studies have also used cattle for studying the characteristics of human disease. Nobuhiro Kajihara et al. found that low glucose conditions exacerbated mtROS production through activation of fatty acid oxidation in bovine aortic endothelial

Indexed in: [Current Contents/Clinical Medicine] [SCI Expanded] [ISI Alerting System] [ISI Journals Master List] [Index Medicus/MEDLINE] [EMBASE/Excerpta Medica] [Chemical Abstracts/CAS]

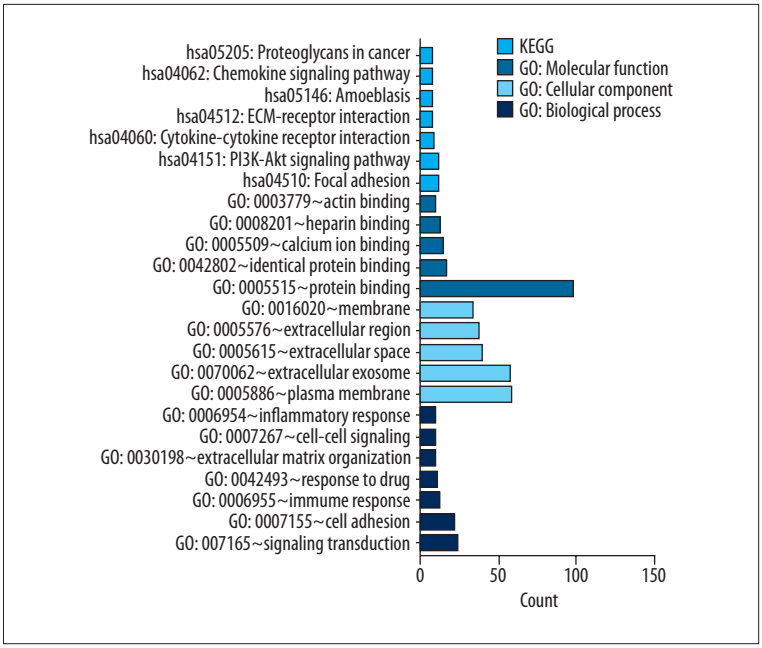

Figure 3. GO and KEGG pathway analyses results of DGEs. GO and KEGG pathway analyses results of DGEs. BP –biological process; CC – cellular component; MF – molecular function; KEGG – Kyoto Encyclopedia of Genes and Genomes. P<0.05.

Table 2. Top 30 in network, ranked by MCC method.

Rank	Name	Score	Rank	Name	Score
1	FN1	6182	16	CCL4	166
2	IGFBP5	5220	17	CXCL16	130
3	APOE	5096	18	CXCL5	129
4	LAMC1	5064	19	CCL19	120
5	CP	5055	19	CXCL14	120
6	SPARCL1	5050	21	TAGLN	93
7	IGFBP7	5043	22	CAV1	68
8	CHRDL1	5041	23	MYH11	64
9	COL1A1	1000	24	MMP1	62
10	TIMP3	940	25	ESR1	55
11	COL1A2	926	26	MGP	50
12	FBLN1	868	27	FLNA	39
13	THBS2	754	28	ADAMTS1	36
14	COL11A1	720	29	AGTR1	31
15	CCR5	184	30	HSP90AA1	25

cells [18]. Other researchers have also used cattle as their own experimental models [19–24]. We used the GSE75240 dataset to show that gut microbes can change the expression of proteins or genes in the blood. The changes in blood vessels can affected by intestinal probiotics, so we used aneurysm datasets from other sites. In this study, we obtained gene expression data from the GSE26969, GSE75436, GSE54083, GSE7084, and GSE75240 datasets, and selected 170 DEGs (containing a gut probiotic dataset and more than 2 of the 4 aneurysms datasets). To further investigate the interactions of these DEGs, we carried out GO term and KEGG pathway analyses. The GO term analysis results indicated that DEGs were mainly enriched

Indexed in: [Current Contents/Clinical Medicine] [SCI Expanded] [ISI Alerting System] [ISI Journals Master List] [Index Medicus/MEDLINE] [EMBASE/Excerpta Medica] [Chemical Abstracts/CAS]

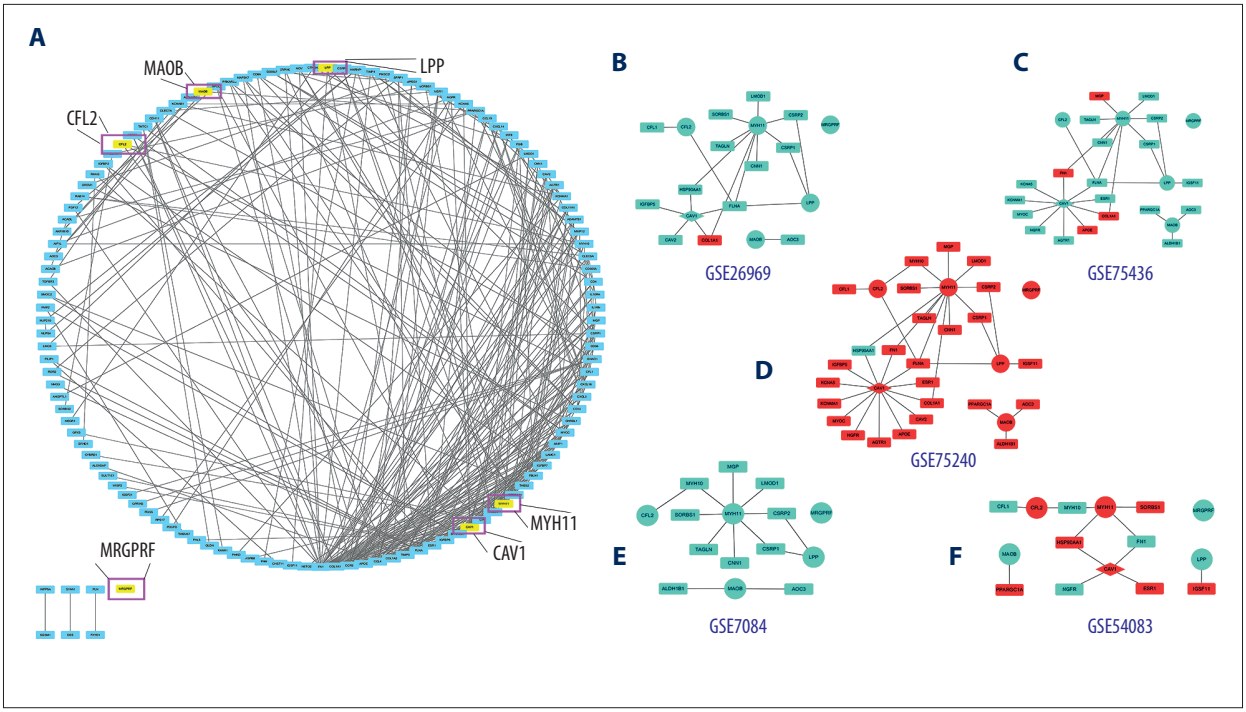

Figure 4. PPI network. (**A**) The PPI networks of 170 DGEs. (**B–F**) Genes related to CFL2, LPP, MYH11, MAOB, MRGPRF, and CAV1 in different GEO datasets. The nodes indicate the genes and the lines represent the corresponding interactions. (**B–F**) Red: up-regulation; Blue: down-regulation. Circle: 5 intersecting DEGs; Diamond: 1 intersecting DEG; Square: others DGEs related to 6 intersecting DEGs

Table 3. List of 6 intersecting DEGs (log FC).

	GSE75240	GSE7084	GSE26969	GSE75436	GSE54083
CFL2	3.71922	–1.75373	–2.58	–1.81832	2.144287
LPP	4.870317	–2.39111	–2.79	–1.55623	–1.92875
MYH11	4.312605	–3.53764	–2.65	–4.71788	1.595093
MAOB	5.841989	–2.05551	–1.78	–3.0551	–2.42214
MRGPRF	5.190016	–1.61803	–2.35	–2.09833	–2.37477
CAV1	5.990843	NA	–1.86	–1.53252	3.940476

NA – not applicable.

in signal transduction, cell adhesion, immune response, extracellular matrix organization, cell-cell signaling, and inflammatory response in the BP terms. The KEGG pathways analysis suggested that DEGs were significantly involved in focal adhesion, PI3K-Akt signaling pathway, cytokine-cytokine receptor interaction, ECM-receptor interaction, amoebiasis, and chemokine signaling pathway. Previous studies showed that the dysfunction of cell adhesion, immune response, inflammatory response, focal adhesion, PI3K-Akt signaling pathway, chemokine signaling pathway, cytokine-cytokine receptor interaction, and ECM-receptor interaction can cause changes in the vascular structure of aneurysms [25–28].

We constructed a Heatmap that clearly shows that CFL2 and MYH11 were upregulated in GSE75240, GSE54083 and downregulated in GSE26969, GSE75436, GSE7084, while LPP, MAOB, and MRGPRF were upregulated in GSE75240 and downregulated in GSE26969, GSE75436, GSE7084, and GSE54083. In general, probiotics can decrease the formation of aneurysms through the increased expression of CFL2, MYH11, LPP, MAOB, and MRGORF, and by inhibiting the formation of IAs through upregulating the expression of CAV1.

PPI of the 170 intersecting DEGs was analyzed based on the STRING database, followed by use of Cytoscape3.6.1 software.

Indexed in: [Current Contents/Clinical Medicine] [SCI Expanded] [ISI Alerting System] [ISI Journals Master List] [Index Medicus/MEDLINE] [EMBASE/Excerpta Medica] [Chemical Abstracts/CAS]

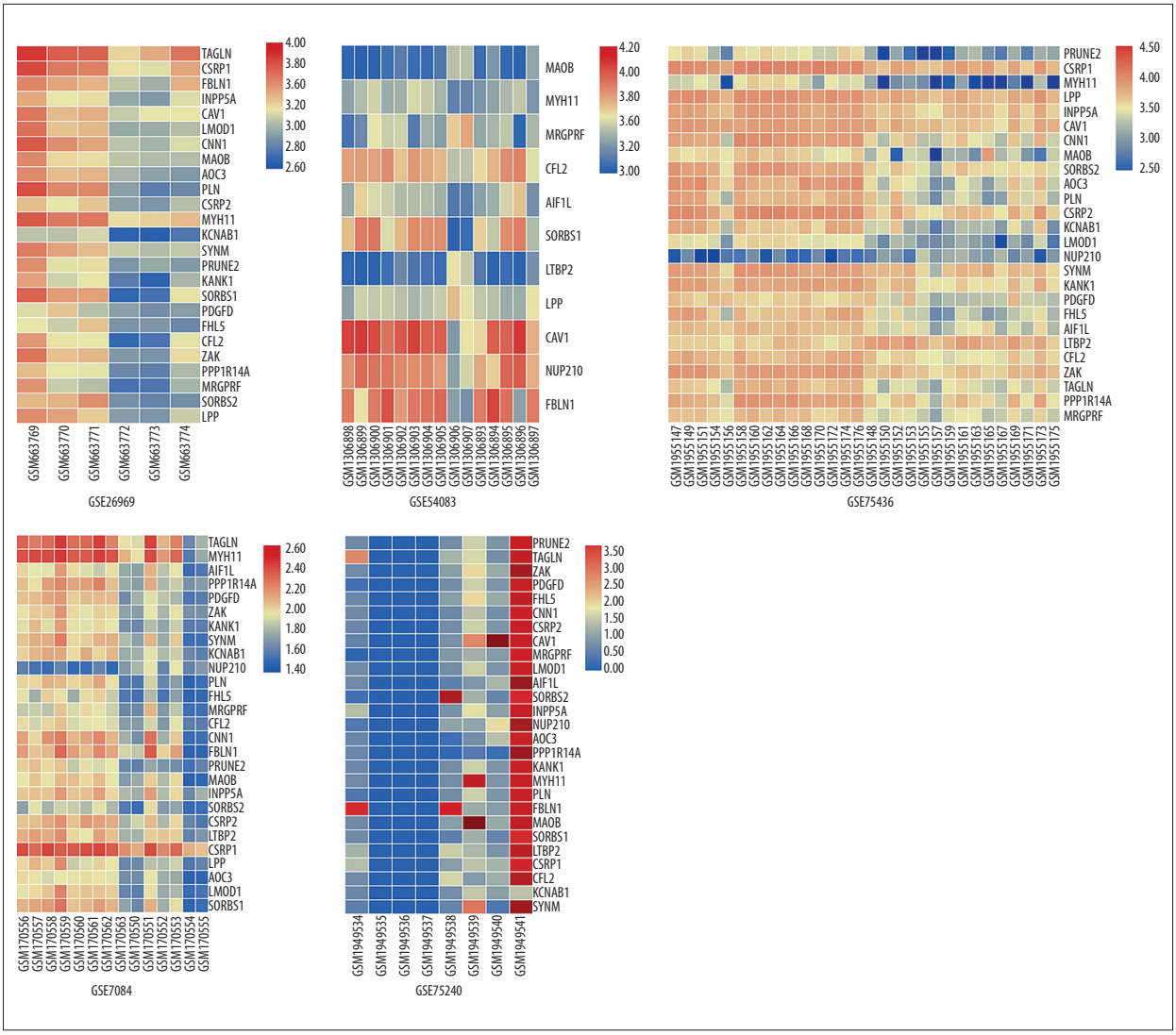

Figure 5. Heatmap of the top DGEs. Heatmap of the 28 DGEs with a fold change of more than 1.5. Red: up-regulation; blue: down-regulation. Normal superficial temporal artery: GSM663769, GSM663770, GSM663771, GSM306898, GSM306899, GSM306900, GSM306901, GSM306902, GSM306903, GSM306904, GSM306905, GSM306906, GSM306907, GSM1955147, GSM1955149, GSM1955151, GSM1955154, GSM1955156, GSM1955158, GSM1955160, GSM1955162, GSM1955164, GSM1955166, GSM1955168, GSM1955170, GSM1955172, GSM1955174, GSM1955176; Intracranial aneurysm: GSM663772, GSM663773, GSM663774, GSM306893, GSM306894, GSM306895, GSM306896, GSM306897, GSM1955148, GSM1955140, GSM1955153, GSM1955155, GSM1955157, GSM1955159, GSM1955161, GSM1955163, GSM1955165, GSM1955167, GSM1955169, GSM1955171, GSM1955173, GSM1955175; Abdominal aorta: GSM170556, GSM170557, GSM170558, GSM170559, GSM170560, GSM170561, GSM170562, GSM170564; Abdominal aortic aneurysm: GSM170563, GSM170550, GSM170551, GSM170552, GSM170553, GSM170554, GSM170555; Gene expression of initial (0day) cow blood sample before supplementation with probiotics: GSM1949534, GSM1949535, GSM1949536, GSM1949537; Gene expression of end of study (60day) cow blood sample after supplementation with probiotics: GSM1949538, GSM1949539, GSM1949540, GSM1949541.

We confirmed 2 candidates for our further study: CAV1 and MYH11. We also found that CFL2, LPP, MYH11, MAOB, and MRGPRF were involved with the association between aneurysm and probiotics, and CAV1 was involved with the associated between IAs and probiotics. CAV1 may be a unique factor in the formation of IAs. CAV1, which is located in cell membrane caveolae, is a member of the caveolin family of proteins [29]. It is generally distributed in smooth-muscle cells, endothelial cells, skeletal myoblasts, and fibroblasts [30]. CAV1 modulates a wide range of cellular events such as proliferation, lipid metabolism, cellular tracking, and signal transduction [29]. MYH11 is a smooth-muscle myosin belonging to the myosin

Indexed in: [Current Contents/Clinical Medicine] [SCI Expanded] [ISI Alerting System] [ISI Journals Master List] [Index Medicus/MEDLINE] [EMBASE/Excerpta Medica] [Chemical Abstracts/CAS]

Table 4. PPI with 6 intersecting DEGs.

CFL2	LPP	MYH11	MAOB	MRGPRF	CAV1
FLNA	FLNA	FLNA	AOC3	NA	FLNA
CFL1	CSRP1	CSRP1	ALDH1B1		ESR1
MYH10	IGSF11	MYH10	PPARGC1A		KCNA5
	CSRP2	CSRP2			KCNMA1
		FN1			FN1
		COL1A1			COL1A1
		HSP90AA1			HSP90AA1
		MGP			AGTR1
		LMOD1			IGFBP5
		SORBS1			NGFR
		CNN1			APOE
		TAGLN			MYOC
					CAV2

NA – not applicable.

heavy chain family, and has been identified as a major contractile protein that converts chemical energy into mechanical energy by the hydrolysis of ATP [31,32]. Previous research, in which MYH11 mutations were found, showed that a structural defect in MYH11 alters smooth-muscle cell phenotype and myosin contractile function, causing an increase of proliferation and aggravating vascular injury [33].

The PPI network analysis clearly shows that FLNA has a strong correlation with CAV1, CFL2, LPP, and MYH11. Protein filamin A (FLNA) helps build extensive internal network of protein filaments in cells, called the cytoskeleton. FLNA can also bind to many other proteins in the cell to carry out various functions, including cell adhesion, migration, and determination of cell shape [34]. FLNA has been found to play roles in regulating skeletal and brain development, the formation of heart tissue and blood vessels, and blood clotting [34–36]. FLNA was lower in the IAs group than in the normal group (log2 (FC)=–2.14 and –1.83, respectively) and was significantly higher in the probiotics-treated group than in the control group (log2 (FC)=4.10). The incidence of aneurysms was reduced by adjusting the interaction between CAV1, CFL2, LPP, MYH11, and FLNA. Further studies are needed to explore the effects of gut probiotics on FLNA and the impact on aneurysm formation.

The above results promote understanding of the molecular mechanism of the pathogenesis of aneurysms, and identify potential therapeutic targets using gut probiotics. The role of these genes in aneurysms, however, is not clear, and further molecular biological experiments are needed to verify these findings.

Conclusions

This bioinformatics analysis identified DEGs obtained from the GEO databases. Using multiple datasets, 6 genes that are associated with probiotics affecting the formation of intracranial aneurysms were identified. Through further analysis of bioinformatics, 2 high-correlation hub genes were confirmed: MYH11 and CAV1. All of these genes were downregulated in aneurysms, and upregulation of these genes was associated with probiotics. These 7 DEGs may be potential targets for aneurysms prevention.

Conflict of interest

None.

Indexed in: [Current Contents/Clinical Medicine] [SCI Expanded] [ISI Alerting System] [ISI Journals Master List] [Index Medicus/MEDLINE] [EMBASE/Excerpta Medica] [Chemical Abstracts/CAS]

Supplementary Data

Supplementary Table 1. List of DGEs considering P<0.05 and |log FC| ≥1.5.

GSE75240		GSE26969		GSE54083		GSE75436		GSE7084	
Gene	Log FC	Gene	Log FC	Gene	Log FC	Gene	Log FC	Gene	Log FC
ACACB	5.01	ACACB	−1.86	AIF1L	1.74	ACACB	−1.68	ACADL	−1.65
ACADL	6.19	ADAMTS1	−2.58	AKR1B10	−4.99	ACADL	−1.71	AGTR1	−1.60
ADAMTS1	6.23	AKR1B10	1.67	ANKRD44	1.70	ADAMTS1	−1.65	AIF1L	−1.56
AGTR1	6.39	ANGPTL1	−2.7	CAV1	3.94	AGTR1	−3.63	ALDH1B1	−1.56
AIF1L	6.00	ANKRD44	−2.25	CCL19	1.79	AIF1L	−2.57	ALOX5AP	1.53
AKR1B10	7.28	AOC3	−2.9	CFL1	−2.58	ALDH1B1	−2.07	AOC3	−2.17
ALDH1B1	6.35	CAV1	−1.86	CFL2	2.14	ALOX5AP	2.22	APOD	−2.31
ALOX5AP	5.10	CAV2	−2.41	CHST11	1.76	ANGPTL1	−4.74	APOE	2.94
ANGPTL1	4.71	CD36	−2.66	CLEC7A	4.92	AOC3	−4.02	BCL11A	1.60
ANKRD44	6.00	CDH11	1.84	CTNNA3	2.52	APOD	−2.31	CAV2	−1.54
AOC3	3.37	CFL1	−2.3	CXCL5	−5.51	APOE	2.67	CCL4	3.16
APOD	5.50	CFL2	−2.58	DIXDC1	4.89	BCL11A	2.16	CCR5	1.63
APOE	4.50	CHRDL1	−2.32	EFHD1	3.68	CAV1	−1.53	CD14	2.16
BCL11A	2.30	CLDND1	−2.72	ERRFI1	1.68	CCL19	−2.11	CD300A	1.73
CAV1	5.99	CNN1	−3.17	ESR1	2.54	CCL4	3.72	CD300LF	1.55
CAV2	4.61	COL11A1	3.59	FBLN1	4.52	CCR5	2.63	CD4	1.66
CCL19	6.29	COL1A1	1.52	FGB	2.42	CD14	2.76	CD8A	1.52
CCL4	2.80	COL1A2	1.51	FGF12	2.39	CD300A	2.45	CFL2	−1.75
CCR5	3.94	CPE	−3.69	FN1	−2.74	CD300LF	2.15	CKMT2	−1.91
CD14	5.19	CRISPLD2	−1.86	GABRA4	3.16	CD36	−3.14	CLEC5A	1.73
CD300A	2.77	CSRP1	−2.74	GALNT3	−1.95	CD4	1.63	CNN1	−2.77
CD300LF	3.70	CSRP2	−1.96	GNAO1	2.30	CD8A	2.30	CP	−1.84
CD36	3.30	CXCL14	−2.67	GPRIN3	1.65	CDH11	2.12	CPE	−2.69
CD4	5.48	CYBRD1	−3.29	HSP90AA1	7.78	CFL2	−1.82	CSRP1	−1.94
CD8A	4.05	DES	−2.24	IGSF11	2.49	CHRDL1	−3.76	CSRP2	−2.40
CDH11	5.21	DIXDC1	−2.37	IGSF21	−1.64	CHST11	2.50	CXCL16	1.67
CFL1	3.86	FBLN1	−1.89	LPP	−1.93	CKMT2	−2.80	CXCL5	2.18
CFL2	3.72	FGB	1.53	LRRC40	2.88	CLDND1	−1.51	CYBRD1	−1.95
CHRDL1	3.47	FHL5	−2.05	LTBP2	−2.39	CLEC5A	3.31	DEF6	1.94
CHST11	4.81	FILIP1	−2.5	MAOB	−2.42	CLEC7A	2.43	EFHD1	−3.38
CKMT2	3.30	FLNA	−2.14	MAP3K7	−1.53	CNN1	−3.27	ERRFI1	−1.72
CLDND1	3.49	GPX3	−3.13	MRGPRF	−2.37	COL11A1	7.24	FBLN1	−2.03
CLEC5A	5.65	GREM1	−3.86	MSR1	3.19	COL1A1	3.21	FHL5	−2.46
CLEC7A	5.65	HNRNPC	−1.51	MYH10	−2.70	COL1A2	1.74	FLVCR2	1.65
CNN1	2.95	HSP90AA1	−3.44	MYH11	1.60	CP	2.76	FXYD1	−1.74
COL11A1	5.32	HSPB8	−1.55	NETO2	−3.24	CRISPLD2	−1.97	GDF15	−1.54
COL1A1	5.08	IGFBP5	−3	NGFR	−2.12	CSRP1	−2.23	GLDN	−1.84
COL1A2	4.10	IGFBP7	−2.23	NMD3	1.59	CSRP2	−2.68	GPX3	−2.87
CP	5.40	INPP5A	−1.67	NRAP	−2.94	CTNNA3	−4.40	HSPB8	−2.04
CPE	6.01	KANK1	−2.65	NUP210	3.22	CXCL14	−4.32	IGFBP2	−2.97

Indexed in: [Current Contents/Clinical Medicine] [SCI Expanded] [ISI Alerting System] [ISI Journals Master List] [Index Medicus/MEDLINE] [EMBASE/Excerpta Medica] [Chemical Abstracts/CAS]

GSE75240		GSE26969		GSE54083		GSE75436		GSE7084	
Gene	Log FC	Gene	Log FC	Gene	Log FC	Gene	Log FC	Gene	Log FC
CRISPLD2	5.12	KCNAB1	–2.37	PDCD7	–2.95	CXCL16	2.48	IGFBP5	–1.53
CSRP1	5.08	LAMC1	–1.88	PIK3CD	–1.82	DEF6	1.66	IGFBP7	–2.01
CSRP2	2.89	LMOD1	–2.8	PMP2	2.93	DES	–5.09	IL10RA	1.73
CTNNA3	5.82	LPP	–2.79	PNN	2.83	ESR1	–2.15	IL1RN	2.86
CXCL14	3.42	LRRC40	–1.9	PNPLA8	1.71	FGF12	–1.95	INPP5A	–1.72
CXCL16	5.14	MAOB	–1.78	PPARGC1A	1.84	FHL5	–3.39	IRF8	1.63
CXCL5	3.60	MAP3K7	–1.51	PRKAR2B	2.56	FILIP1	–2.18	KANK1	–2.28
CYBRD1	4.78	MPP7	–2.33	RAB14	–2.66	FLNA	–1.83	KCNA5	–3.29
DEF6	5.52	MRGPRF	–2.35	RHAG	3.09	FLVCR2	2.26	KCNAB1	–2.38
DES	6.00	MYH11	–2.65	ROR2	–1.81	FN1	2.06	KCNMA1	–1.93
DIXDC1	4.54	NEGR1	–2.47	RPS17	2.24	FXYD1	–1.50	LAMC1	–1.80
EFHD1	5.22	NMD3	–1.5	SGSM1	2.28	GABRA4	–1.87	LMO3	–2.50
ERRFI1	2.96	NUP54	–1.6	SMPDL3A	2.56	GALNT3	1.84	LMOD1	–2.86
ESR1	4.29	PDCD7	–1.77	SORBS1	4.45	GDF15	2.31	LPP	–2.39
FBLN1	5.19	PDE5A	–2.07	STAC	1.80	GLDN	–2.90	LTBP2	–2.00
FGB	5.53	PDGFD	–1.66	SULT1E1	1.71	GNAO1	–2.10	MAOB	–2.06
FGF12	4.16	PDLIM3	–2.33	TIMP3	2.56	GPRIN3	2.07	MGP	–2.51
FHL5	5.73	PGM5	–2.57	TMEM169	–1.59	GREM1	2.80	MMP1	1.59
FILIP1	3.32	PLN	–5.01	ZNF280B	1.77	HNRNPC	1.55	MMP12	2.70
FLNA	4.10	PLSCR4	–2.8			IGFBP2	2.42	MPEG1	2.51
FLVCR2	2.48	PNN	–1.73			IGSF11	–3.31	MRAP2	–3.66
FN1	7.15	PNPLA8	–2.45			IGSF21	1.75	MRGPRF	–1.62
FXYD1	4.48	PPP1R14A	–2.17			IL10RA	1.80	MYH10	–3.62
GABRA4	5.61	PRKAR2B	–2.32			IL1RN	2.31	MYH11	–3.54
GALNT3	4.44	PRR11	–2.31			INPP5A	–1.61	MYOC	–1.74
GDF15	4.98	PRUNE2	–2.43			IRF8	1.75	NOV	–3.26
GLDN	5.70	RAB14	–1.86			KANK1	–2.06	NUP210	1.59
GNAO1	3.35	RASSF3	–3.17			KCNA5	–4.42	PDGFD	–2.78
GPRIN3	3.90	RGS5	–2.35			KCNAB1	–3.42	PDLIM3	–2.82
GPX3	5.12	RNASE1	–1.72			KCNMA1	–2.49	PIK3CD	1.99
GREM1	5.02	RPS17	–1.97			LMO3	–2.38	PLAC8	1.63
HNRNPC	4.61	SERPING1	–2.19			LMOD1	–3.19	PLN	–3.28
HSP90AA1	–3.60	SFRP1	–1.99			LPP	–1.56	PLSCR4	–1.62
HSPB8	5.57	SMOC2	–2.48			LTBP2	1.54	PNKD	1.58
IGFBP2	3.58	SORBS1	–4.15			MAOB	–3.06	PPP1R14A	–2.63
IGFBP5	4.43	SORBS2	–3.51			MGP	2.20	PRUNE2	–2.61
IGFBP7	3.50	SPARCL1	–2.56			MMP1	2.32	RBPMS	–2.20
IGSF11	2.78	SRPX	–2.67			MMP12	1.98	RCAN2	–3.16
IGSF21	3.24	SYNM	–2.44			MPEG1	2.14	RGS5	–3.42
IL10RA	2.78	TAGLN	–2.54			MPP7	–3.58	RNASE1	1.67
IL1RN	6.21	TCEAL4	–2.97			MRAP2	–1.56	SCARA3	–1.67
INPP5A	3.63	TGFBR3	–2.01			MRGPRF	–2.10	SERPING1	–2.03
IRF8	5.86	TIMP3	–2.01			MSR1	3.35	SLC37A2	1.93
KANK1	3.89	TMEM47	–2.52			MYH11	–4.72	SLCO2B1	1.67

Indexed in: [Current Contents/Clinical Medicine] [SCI Expanded] [ISI Alerting System] [ISI Journals Master List] [Index Medicus/MEDLINE] [EMBASE/Excerpta Medica] [Chemical Abstracts/CAS]

GSE75240		GSE26969		GSE54083		GSE75436		GSE7084	
Gene	Log FC	Gene	Log FC	Gene	Log FC	Gene	Log FC	Gene	Log FC
KCNA5	4.74	TMTC1	−1.67			MYOC	−4.14	SMOC2	−2.86
KCNAB1	2.95	ZAK	−2.74			NEGR1	−2.23	SNX10	2.22
KCNMA1	3.39					NETO2	2.28	SORBS1	−3.16
LAMC1	3.59					NGFR	−1.57	SORBS2	−1.52
LMO3	3.12					NOV	−3.14	SPARCL1	−3.06
LMOD1	3.06					NRAP	−2.27	SRPX	−1.93
LPP	4.87					NUP210	1.86	SYNM	−2.49
LRRC40	4.39					NUP54	−1.61	TAGLN	−3.01
LTBP2	5.15					PDE5A	−1.58	TCEAL4	−1.85
MAOB	5.84					PDGFD	−1.91	TGFBR3	−1.96
MAP3K7	5.05					PGM5	−3.02	THBS2	−2.57
MGP	5.97					PLAC8	2.26	TIMP4	−1.62
MMP1	4.57					PLN	−3.07	TMEM47	−3.01
MMP12	6.16					PMP2	−3.58	TSPAN33	1.70
MPEG1	4.02					PNKD	2.24	WISP2	−2.09
MPP7	4.65					PPARGC1A	−1.68	ZAK	−1.85
MRAP2	5.45					PPP1R14A	−2.16		
MRGPRF	5.19					PRR11	1.71		
MSR1	4.34					PRUNE2	−3.87		
MYH10	4.89					RASSF3	−2.12		
MYH11	4.31					RBPMS	−2.21		
MYOC	3.88					RCAN2	−1.72		
NEGR1	3.15					RHAG	−2.59		
NETO2	2.77					ROR2	2.05		
NGFR	4.62					SCARA3	−2.17		
NMD3	2.96					SFRP1	−2.93		
NOV	6.11					SGSM1	−1.75		
NRAP	4.85					SLC37A2	1.51		
NUP210	4.76					SLCO2B1	2.77		
NUP54	4.12					SMPDL3A	1.54		
PDCD7	4.38					SNX10	1.94		
PDE5A	6.51					SORBS2	−2.71		
PDGFD	3.20					STAC	−2.66		
PDLIM3	3.76					SULT1E1	2.27		
PGM5	5.00					SYNM	−1.69		
PIK3CD	2.66					TAGLN	−2.31		
PLAC8	6.22					THBS2	1.91		
PLN	3.39					TIMP4	−2.13		
PLSCR4	4.04					TMEM169	1.57		
PMP2	6.15					TMTC1	−1.62		
PNKD	5.77					TSPAN33	1.59		
PNN	5.23					WISP2	−4.84		
PNPLA8	2.97					ZAK	−1.93		
PPARGC1A	5.22					ZNF280B	1.88		

Indexed in: [Current Contents/Clinical Medicine] [SCI Expanded] [ISI Alerting System] [ISI Journals Master List] [Index Medicus/MEDLINE] [EMBASE/Excerpta Medica] [Chemical Abstracts/CAS]

GSE75240		GSE26969		GSE54083		GSE75436		GSE7084	
Gene	Log FC	Gene	Log FC	Gene	Log FC	Gene	Log FC	Gene	Log FC
PPP1R14A	3.77								
PRKAR2B	4.79								
PRR11	2.70								
PRUNE2	5.93								
RAB14	–3.28								
RASSF3	4.94								
RBPMS	3.96								
RCAN2	3.42								
RGS5	7.11								
RHAG	5.03								
RNASE1	4.97								
ROR2	4.97								
RPS17	4.36								
SCARA3	3.58								
SERPING1	5.94								
SFRP1	5.46								
SGSM1	4.44								
SLC37A2	5.00								
SLCO2B1	5.05								
SMOC2	4.96								
SMPDL3A	4.21								
SNX10	4.75								
SORBS1	3.91								
SORBS2	4.13								
SPARCL1	3.31								
SRPX	5.76								
STAC	4.51								
SULT1E1	4.90								
SYNM	5.98								
TAGLN	4.45								
TCEAL4	–2.02								
TGFBR3	3.51								
THBS2	3.75								
TIMP3	5.40								
TIMP4	5.95								
TMEM169	2.84								
TMEM47	4.99								
TMTC1	4.60								
TSPAN33	3.69								
WISP2	4.37								
ZAK	2.34								
ZNF280B	3.05								

Indexed in: [Current Contents/Clinical Medicine] [SCI Expanded] [ISI Alerting System] [ISI Journals Master List] [Index Medicus/MEDLINE] [EMBASE/Excerpta Medica] [Chemical Abstracts/CAS]

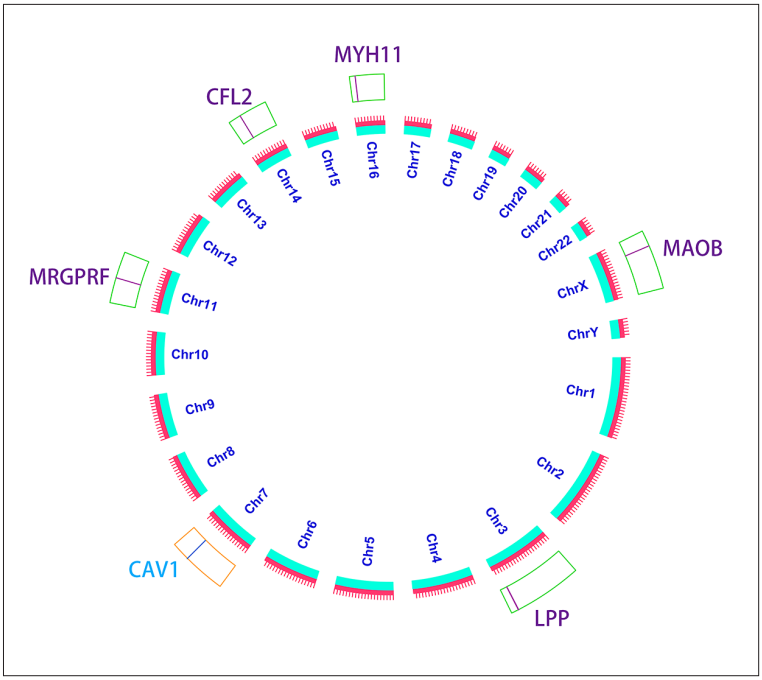

Supplementary Figure 1. The location of DGEs on the chromosome. 6 intersecting DEGs are located at different positions on the chromosome. Blue: intersection of IAs and probiotics; Purple: intersection of aneurysms and probiotics

References:

1. Macdonald RL, Schweizer TA: Spontaneous subarachnoid haemorrhage. Lancet (London, England), 2017; 389(10069): 655–66
2. Mohan D, Munteanu V, Coman T, Ciurea AV: Genetic factors involves in intracranial aneurysms – actualities. J Med Life, 2015; 8(3): 336–41
3. Frösen J, Tulamo R, Paetau A et al: Saccular intracranial aneurysm: pathology and mechanisms. Acta Neuropathol, 2012; 123(6): 773–86
4. Kanematsu Y, Kanematsu M, Kurihara C et al: Critical roles of macrophages in the formation of intracranial aneurysm. Stroke, 2011; 42(1): 173–78
5. Koeth RA, Wang Z, Levison BS et al: Intestinal microbiota metabolism of L-carnitine, a nutrient in red meat, promotes atherosclerosis. Nat Med, 2013; 19(5): 576–85
6. Holmes E, Li JV, Marchesi JR, Nicholson JK: Gut microbiota composition and activity in relation to host metabolic phenotype and disease risk. Cell Metab, 2012; 16(5): 559–64
7. Shikata F, Shimada K, Sato H et al: Potential influences of gut microbiota on the formation of intracranial aneurysm. Hypertension (Dallas, Tex: 1979), 2019; 73(2): 491–96
8. Li L, Yang X, Jiang F et al: Transcriptome-wide characterization of gene expression associated with unruptured intracranial aneurysms. Eur Neurol, 2009; 62(6): 330–37
9. Nakaoka H1, Tajima A, Yoneyama T et al: Gene expression profiling reveals distinct molecular signatures associated with the rupture of intracranial aneurysm. Stroke, 2014; 45(8): 2239–45
10. Lenk GM1, Tromp G, Weinsheimer S et al: Whole genome expression profiling reveals a significant role for immune function in human abdominal aortic aneurysms. BMC Genomics, 2007; 8: 237
11. Adjei-Fremah S, Ekwemalor K, Asiamah E et al: Transcriptional profiling of the effect of lipopolysaccharide (LPS) pretreatment in blood from probiotics-treated dairy cows. Genom Data, 2016; 10: 15–18
12. Zhang JZ, Wu ZH, Cheng Q: Screening and identification of key biomarkers in nasopharyngeal carcinoma: Evidence from bioinformatic analysis. Medicine, 2019; 98(48): e17997
13. Davis S, Meltzer PS: GEOquery: A bridge between the Gene Expression Omnibus (GEO) and BioConductor. Bioinformatics (Oxford, England), 2007; 23(14): 1846–47
14. Huang da W, Sherman BT, Lempicki RA: Systematic and integrative analysis of large gene lists using DAVID bioinformatics resources. Nat Protoc, 2009; 4(1): 44–57
15. Szklarczyk D, Morris JH, Cook H et al: The STRING database in 2017: Quality-controlled protein-protein association networks, made broadly accessible. Nucleic Acids Res, 2017; 45: D362–68
16. Shannon P, Markiel A, Ozier O et al: Cytoscape: A software environment for integrated models of biomolecular interaction networks. Genome Res, 2003; 13(11): 2498–504
17. Elsik CG, Tellam RL, Worley KC et al: The genome sequence of taurine cattle: A window to ruminant biology and evolution. Science (New York, NY), 2009; 324(5926): 522–28
18. Kajihara N, Kukidome D, Sada K et al: Low glucose induces mitochondrial reactive oxygen species via fatty acid oxidation in bovine aortic endothelial cells. J Diabetes Investig, 2017; 8(6): 750–61
19. Fujie T, Murakami M, Yoshida E et al: Transcriptional induction of metallothionein by Tris(pentafluorophenyl)stibane in cultured bovine aortic endothelial cells. Int J Mol Sci, 2016; 17(9): pii: E1381
20. Qu L, Yu L, Wang Y et al: Inward rectifier K+ currents are regulated by CaMKII in endothelial cells of primarily cultured bovine pulmonary arteries. PLoS One, 2015; 10(12): e0145508
21. Fujie T, Takenaka F, Yoshida E et al: Possible mechanisms underlying transcriptional induction of metallothionein isoforms by tris(pentafluorophenyl) stibane, tris(pentafluorophenyl)arsane, and tris(pentafluorophenyl)phosphane in cultured bovine aortic endothelial cells. J Toxicol Sci, 2019; 44(5): 327–33
22. Chandra S, Fulton DJR, Caldwell RB: Hyperglycemia-impaired aortic vasorelaxation mediated through arginase elevation: Role of stress kinase pathways. Eur J Pharmacol, 2019; 844: 26–37
23. Chang S, Lanctot AC, McCarter MD: The prediction of radiofrequency ablation zone volume using vascular indices of 3-dimensional volumetric colour Doppler ultrasound in an *in vitro* blood-perfused bovine liver model. Br J Radiol, 2017; 90(1070): 20160661
24. Chung KY, Smith SB, Choi SH, Johnson BJ: Oleic acid enhances G protein coupled receptor 43 expression in bovine intramuscular adipocytes but not in subcutaneous adipocytes. J Anim Sci, 2016; 94(5): 1875–83
25. Liu P, Shi Y, Fan Z et al: Inflammatory smooth muscle cells induce endothelial cell alterations to influence cerebral aneurysm progression via regulation of integrin and VEGF expression. Cell Transplant, 2019; 28(6): 713–22
26. Erhart P, Cakmak S, Grond-Ginsbach C et al: Inflammasome activity in leucocytes decreases with abdominal aortic aneurysm progression. Int J Mol Med, 2019; 44(4): 1299–308

Indexed in: [Current Contents/Clinical Medicine] [SCI Expanded] [ISI Alerting System] [ISI Journals Master List] [Index Medicus/MEDLINE] [EMBASE/Excerpta Medica] [Chemical Abstracts/CAS]

27. Wang Z, Guo J, Han X et al: Metformin represses the pathophysiology of AAA by suppressing the activation of PI3K/AKT/mTOR/autophagy pathway in ApoE(–/–) mice. Cell biosci, 2019; 9: 68
28. Wang Y, Jia L, Xie Y et al: Involvement of macrophage-derived exosomes in abdominal aortic aneurysms development. Atherosclerosis, 2019; 289: 64–72
29. Huang Q, Zhong W, Hu Z, Tang X: A review of the role of cav-1 in neuropathology and neural recovery after ischemic stroke. J neuroinflammation, 2018; 15(1): 348
30. Anderson RG: The caveolae membrane system. Ann Rev Biochem, 1998; 67: 199–225
31. Zhu L, Vranckx R, Khau Van Kien P et al: Mutations in myosin heavy chain 11 cause a syndrome associating thoracic aortic aneurysm/aortic dissection and patent ductus arteriosus. Nat Genet, 2006; 38(3): 343–49
32. Milewicz DM, Trybus KM, Guo DC et al: Altered smooth muscle cell force generation as a driver of thoracic aortic aneurysms and dissections. Arterioscler Thromb Vasc Biol, 2017; 37(1): 26–34
33. Kuang SQ, Kwartler CS, Byanova KL et al: Rare, nonsynonymous variant in the smooth muscle-specific isoform of myosin heavy chain, MYH11, R247C, alters force generation in the aorta and phenotype of smooth muscle cells. Circ Res, 2012; 110(11): 1411–22
34. Falet H: New insights into the versatile roles of platelet FlnA. Platelets, 2013; 24(1): 1–5
35. Hart AW, Morgan JE, Schneider J et al: Cardiac malformations and midline skeletal defects in mice lacking filamin A. Hum Mol Genet, 2006; 15(16): 2457–67
36. Feng Y, Chen MH, Moskowitz IP et al: Filamin A (FLNA) is required for cell-cell contact in vascular development and cardiac morphogenesis. Proc Natl Acad Sci USA, 2006; 103(52): 19836–41

Indexed in: [Current Contents/Clinical Medicine] [SCI Expanded] [ISI Alerting System] [ISI Journals Master List] [Index Medicus/MEDLINE] [EMBASE/Excerpta Medica] [Chemical Abstracts/CAS]